8
Quasi-one-dimensional surface plasmons

Figures

8.2 Propagating surface plasmons on metallic wires of circular cross section

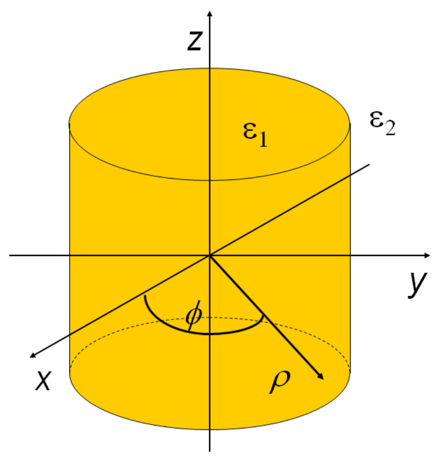

Fig. 8.1. Cylindrical nanowire along the *z*-direction.

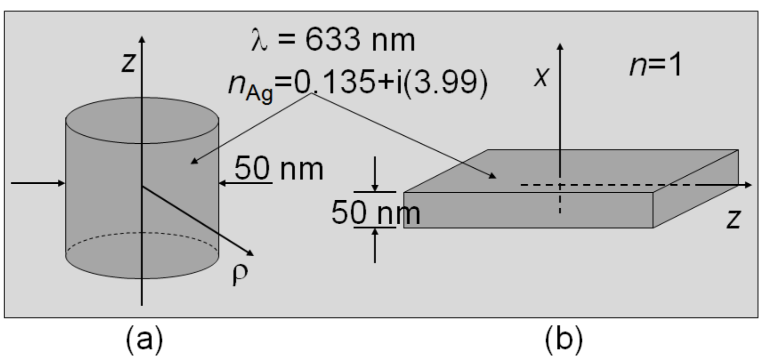

Fig. 8.2. (a) Cylindrical silver nanowire in air and (b) 50 nm silver film in air.

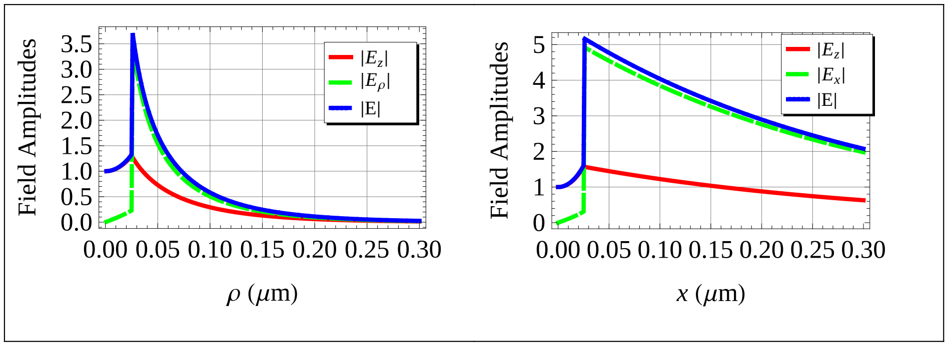

Fig. 8.3. (Left) The fields of a propagating SP mode on the cylindrical silver nanowire shown in Fig. 8.2(a) are plotted as a function of the radial distance, ρ, from the center of the cylinder. The effective index of the SP is 1.604 + 0.0416 i. (Right) The fields of a propagating SP mode on a planar silver film shown in Fig. 8.2(b) are plotted as a function of the distance along the normal to the surface, x, from the center of the film. The effective index of the SP is 1.055 + 0.00567 i. (*Mathematica* simulation)

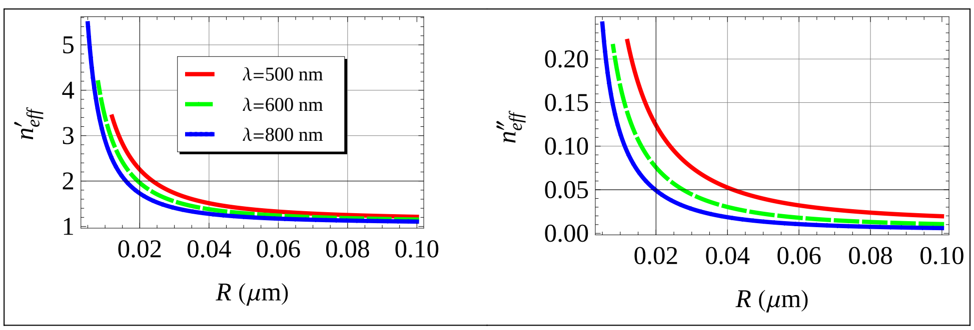

Fig. 8.4. (Left) n'_{eff} and (right) n''_{eff} of the SP are plotted as a function of the radius, R, of the cylindrical silver nanowire at wavelengths of 500 nm (solid), 600 nm (dashes) and 800 nm (dots). (*Mathematica* simulation)

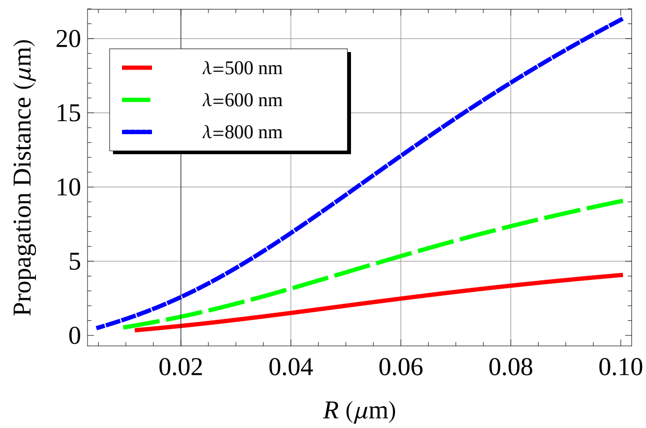

Fig. 8.5. The propagation distance of a SP along a cylindrical silver nanowire is a strong function of the radius of the cylinder, *R*, and decreases as the radius decreases. These results are for wavelengths of 500 nm (solid line), 600 nm (dashes) and 800 nm (dots). (*Mathematica* simulation)

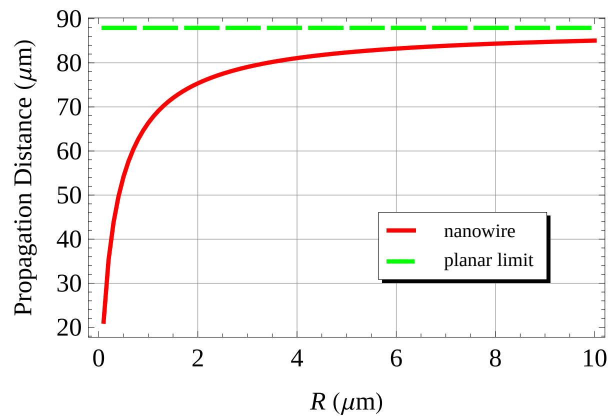

Fig. 8.6. The propagation distance of a SP on a cylindrical wire (solid line) approaches that of a planar surface (dashes) in the limit of a wire with a very large radius. (*Mathematica* simulation)

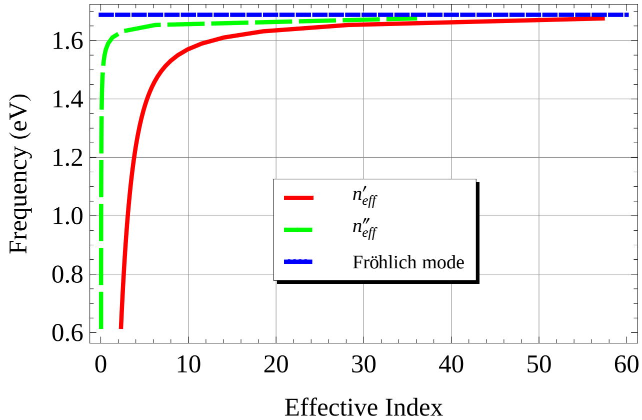

Fig. 8.7. The SP dispersion curve is computed for a Drude metal nanowire with a radius of 50 nm. The Drude parameters are $\omega_p = 15\,\text{eV}$ and $\gamma = 0.1$ eV. Both n'_{eff} (solid line) and n''_{eff} (dashes) are plotted, as well as the frequency of the Fröhlich mode (dots), $\omega_p \big/ \left(2\,\pi\,\sqrt{2}\right)$, which is the asymptotic limit. (*Mathematica* simulation)

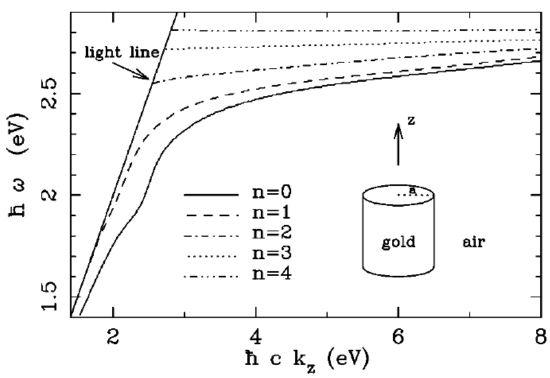

Fig. 8.8. Dispersion curves for SP modes on a gold cylinder with a diameter of 200 nm surrounded by air. Reprinted with permission from U. Schröter and A. Dereux, *Phys. Rev. B* **64** 125420 (2001). © 2001 by the American Physical Society. [4]

8.3 Propagating surface plasmons on metallic wires of noncircular cross section

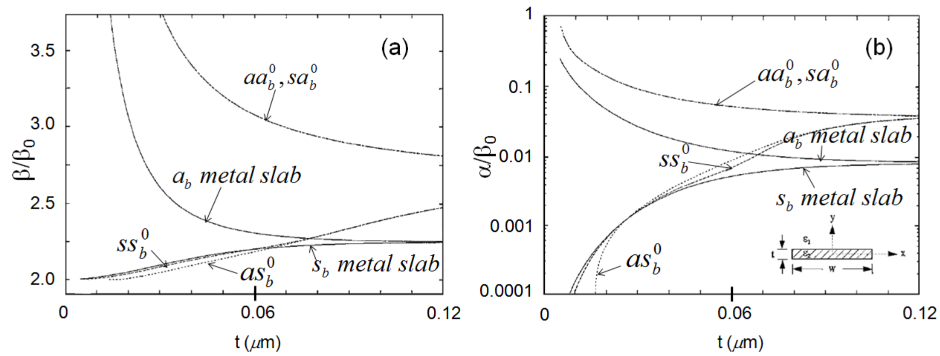

Fig. 8.9. (a) n'_{eff} and (b) n''_{eff} as a function of nanowire thickness for SP modes on a silver rectangular nanowire surrounded by a dielectric with a refractive index of 2. The wavelength is 633 nm and the dielectric constant for silver is -19 + i 0.53. The width, w, of the wire is 1 μm. The results for the infinitely wide slab are also plotted. Used by permission. [6]

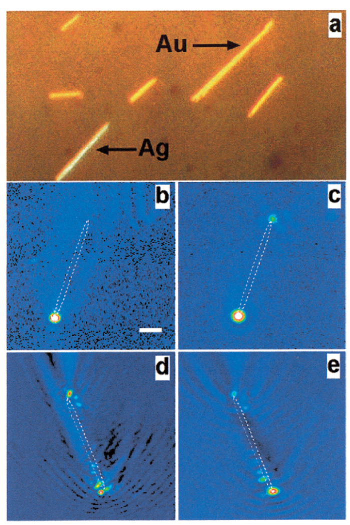

Fig. 8.10. Evidence for SP propagation along a nanowire. Silver and gold nanowires are shown in (a). Light at a wavelength of 532 nm is focused on the bottom end of a gold nanowire in (b) and a silver nanowire in (c). Light is emitted only from the other end of the silver nanowire. However, light at a wavelength of 820 nm is focused at the bottom end of a gold nanowire in (d) and a silver nanowire in (e) and in this case light is emitted at the other end of both nanowires. Reprinted with permission from [10]. © 2000 American Chemical Society.

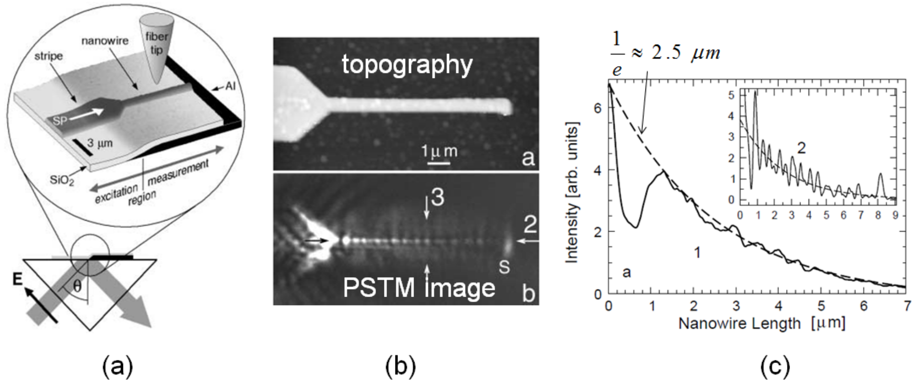

Fig. 8.11. Kretschmann technique for launching a SP mode on a nanowire. The experimental setup is shown in (a) and described in the text. The upper image in (b) is an AFM scan of the nanowire. The bottom image is from a photon scanning tunneling microscope image showing the intensity of the SP as it propagates down the nanowire. The main graph in (c) is a scan of light intensity along the nanowire. The inset is a light intensity scan along a shorter 8 μm nanowire in which there is a partial reflection of the SP from the end of the wire which generates interference fringes with the forward propagating SP. Used by permission. [12]

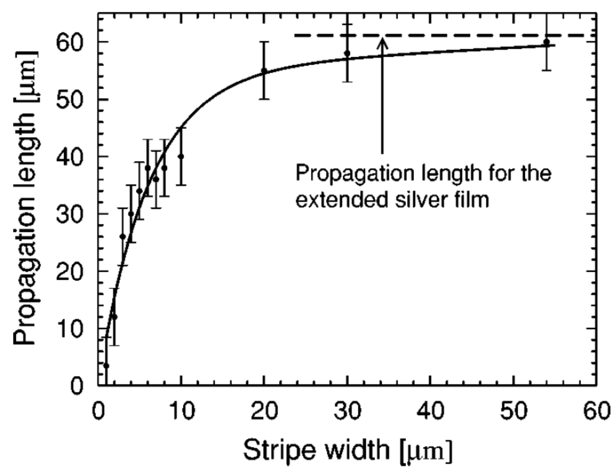

Fig. 8.12. Propagation distance of SPs on a 70 nm thick silver stripe at a wavelength of 633 nm for various stripe widths. The dashed line in the figure is simply a guide to the eye. Reprinted with permission from B. Lamprecht, J. R. Krenn, H. Ditlbacher, M. Salerno, N. Felidj, A. Leitner, F. R. Aussenegg and J. C. Weeber, *Appl. Phys. Lett.* **79** #1, 51-53 (2001). © 2001, American Institute of Physics. [13]

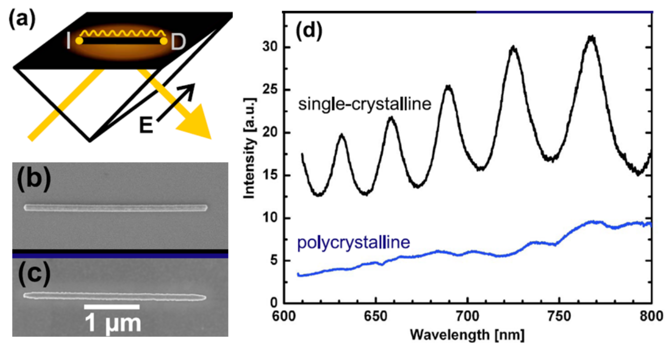

Fig. 8.13. (a) Geometry for excitation of the SP in the nanowire. The silver nanowire is located on a prism face and white light is focused through the prism onto the entire nanowire, but only couples to the SP at the input end labelled "I." The SP propgates towards the distal end, "D." (b) SEM micrograph of the chemically prepared nanowire. (c) SEM micrograph of the lithographically defined nanowire. (d) The spectrum of the light scattered from the two nanowires. Reprinted with permission from H. Ditlbacher, A. Hohenau, D. Wagner, U. Kriebig, M. Rogers, F. Hofer, F. R. Aussenegg and J. R. Krenn, *Phys. Rev. Lett.* **95** 257403 (2005). © 2005 by the American Physical Society. [14]

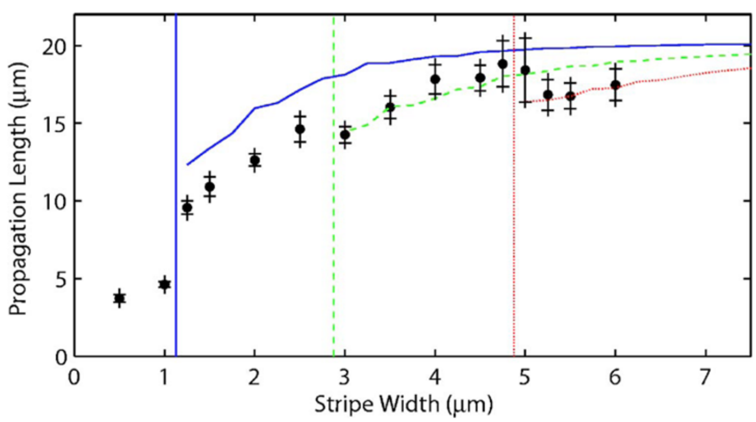

Fig. 8.14. Circular dots are experimental measurements of SP propagation distance for different wire widths. The solid, dashed, and dotted lines are calculated SP propagation distances for the first three SP modes of the wire. The vertical lines are the predicted cutoff wire widths. Reprinted with permission from R. Zia, J. A. Schuller and M. L. Brongersma, *Phys. Rev. B* **74** 165415 (2006). © 2006 by the American Physical Society. [15]

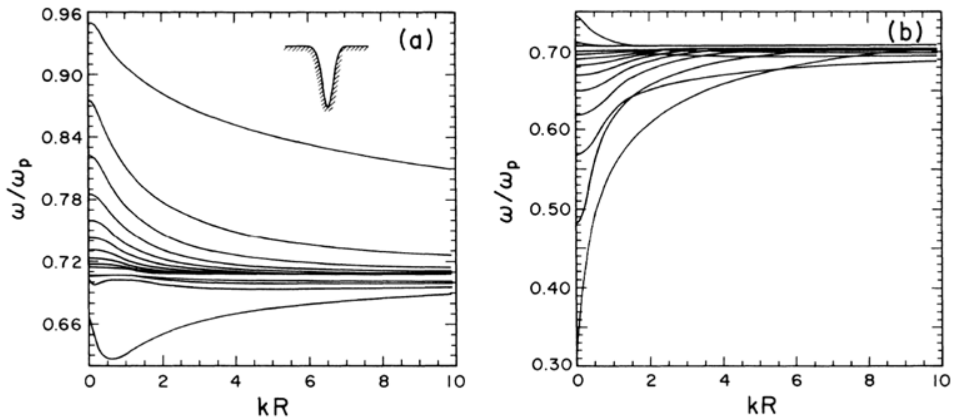

Fig. 8.15. SP dispersion curves for a channel with Gaussian surface profile y = -A $\exp\left(-x^2/R^2\right)$ where A/R = 8. Modes are plotted for which the potential is (a) an even function of x and (b) and odd function of x. Reprinted with permission from J. Q. Lu and A. A. Maradudin, *Phys. Rev. B* **42** 11159-11165 (1990). © 1990 by the American Physical Society. [20]

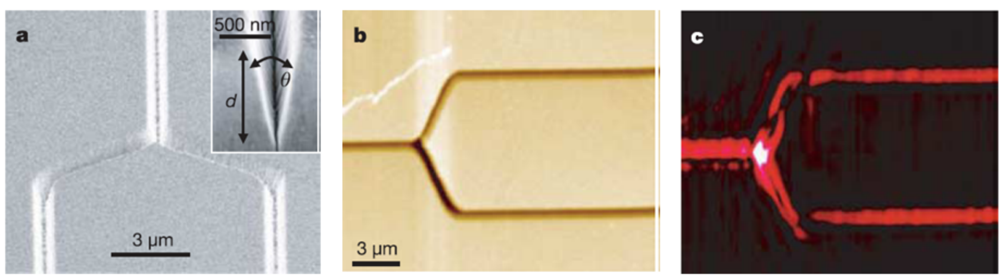

Fig. 8.16. (a) Optical image of a V-groove in a gold film designed as a Y-splitter. The inset is the groove profile. (b) Topographical image. (c) Near field optical image of light at a wavelength of 1600 nm propagating from left to right. Reprinted by permission from Macmillan Publishers Ltd: *Nature* [23] © 2006.

8.4 Propagating surface plasmons on hollow cylindrical waveguides

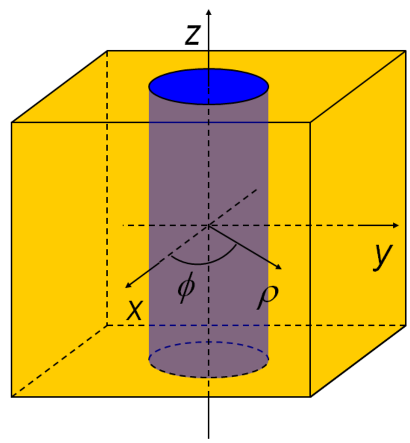

Fig. 8.17. Cylindrical waveguide consisting of hollow metal tube with an inner dielectric.

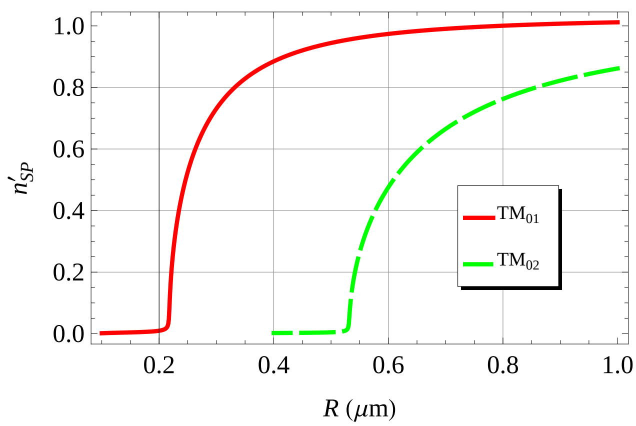

Fig. 8.18. Dependence of the effective SP refractive index, n'_{eff}, for the first two n = 0 SP modes of a hollow silver waveguide filled with air on the radius at a wavelength of 633 nm. The refractive index of the silver is 0.135 + 3.99 i. (*Mathematica* simulation)

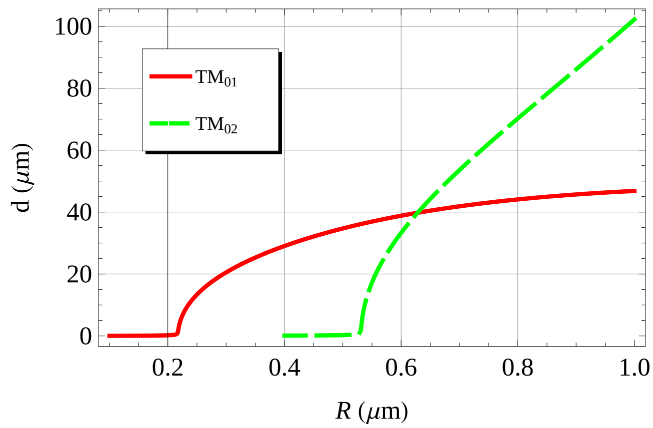

Fig. 8.19. Dependence on waveguide radius of the 1/*e* propagation distance for the first two n = 0 SP modes of a hollow silver waveguide filled with air at a wavelength of 633 nm. The refractive index of the silver is 0.135 + 3.99 i. (*Mathematica* simulation)

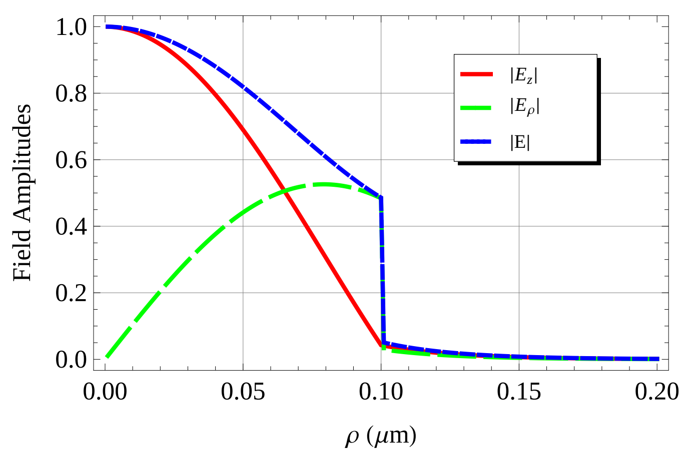

Fig. 8.20. Fields of a hollow silver waveguide filled with air with a 200 nm core diameter at a wavelength of 633 nm as a function of radial position, ρ. The index of the silver is 0.135 + 3.99 i and the effective index for the SP mode is 0.00146 + 2.117 i. (*Mathematica* simulation)

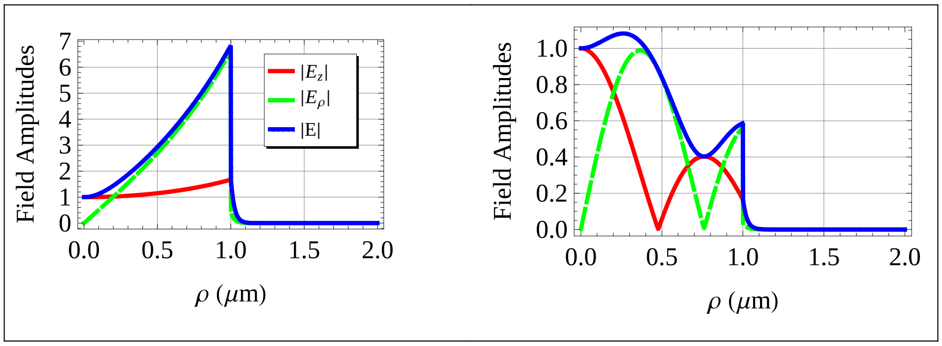

Fig. 8.21. Dependence on radius of the fields for the first (left) and second (right) n = 0 SP modes for a silver tube with a 1 μm radius and air inside at a wavelength of 633 nm. The index of the silver is 0.135 + 3.99 i. The effective SP index for the first mode is 1.0117 + 0.00215 i. The effective SP index for the second mode is 0.8617 + 0.000986 i. (*Mathematica* simulation)

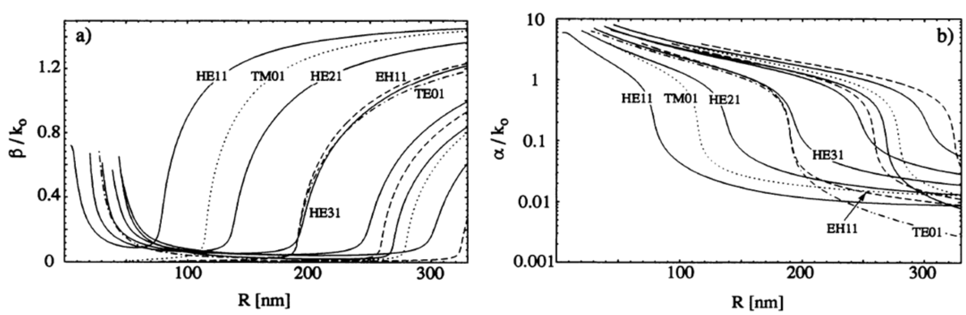

Fig. 8.22. (a) n'_{eff} and (b) n''_{eff} for a cylindrical aluminum waveguide at a wavelength of 488 nm as a function of core radius. The dielectric constant for the core is 2.16 and the dielectric constant for the aluminum is -34 + 8.5 i. Reprinted with permission from L.Novotny and C. Hafner, *Phys. Rev. E* **50** 4094-4106 (1994). © 1994 by the American Physical Society. [25]

8.5 Propagating surface plasmons on hollow cylindrical shells

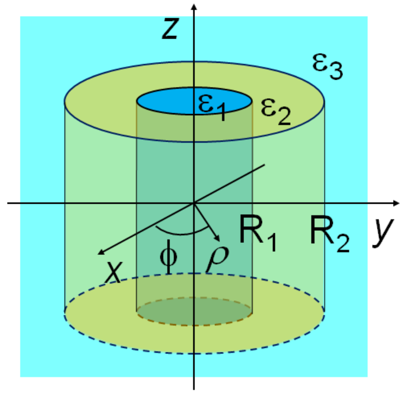

Fig. 8.23. Cylindrical metallic shell with a dielectric on the inside and outside.

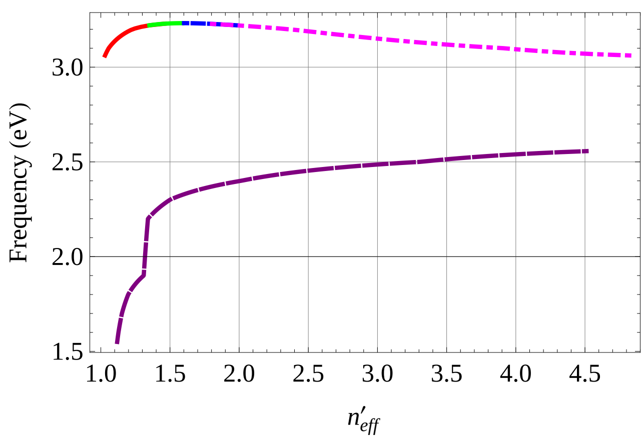

Fig. 8.24. SP dispersion curve for a lossless cylindrical metallic shell as described in the text after Ref. [4]. (*Mathematica* simulation)

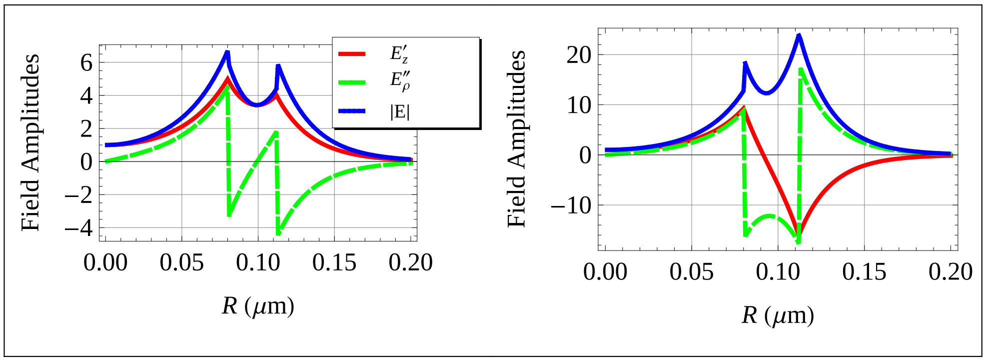

Fig. 8.25. SP fields for the two n = 0 modes with n_{eff} = 3.3 on the dispersion curve of Fig. 8.22. The fields for the lower energy mode are shown on the left and the higher energy mode on the right. (*Mathematica* simulation)

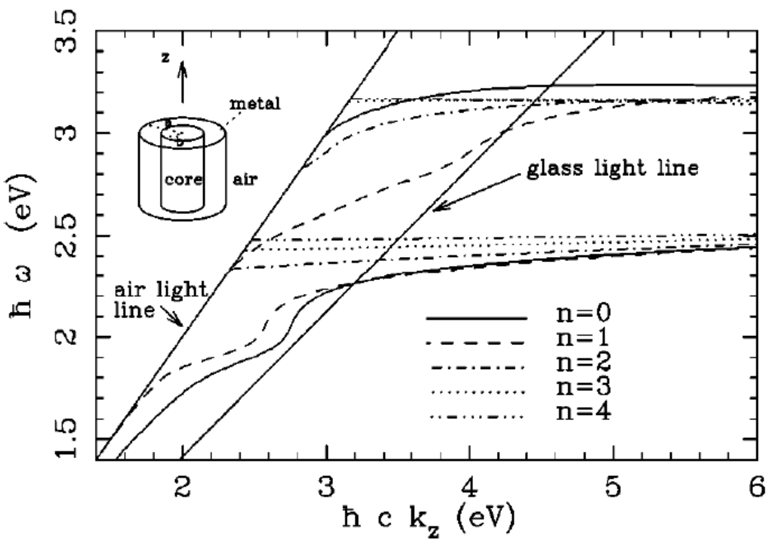

Fig. 8.26. Dispersion curves for both high and low energy SP modes for the first four azimuthal indices. Reprinted with permission from U.Schröter and A. Dereux, *Phys. Rev. B* **64** 125420 (2001). © 2001 by the American Physical Society. [4]

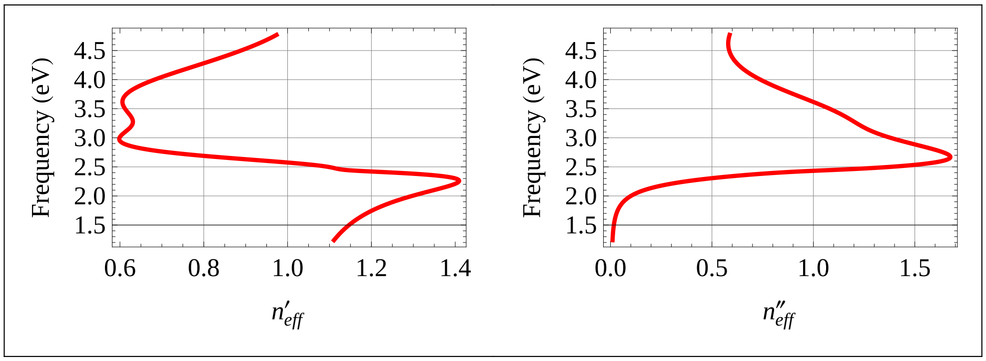

Fig. 8.27. Real part (left) and imaginary part (right) of the SP dispersion for a gold cylindrical shell with the same dimensions as in Fig. 8.25. (*Mathematica* simulation)

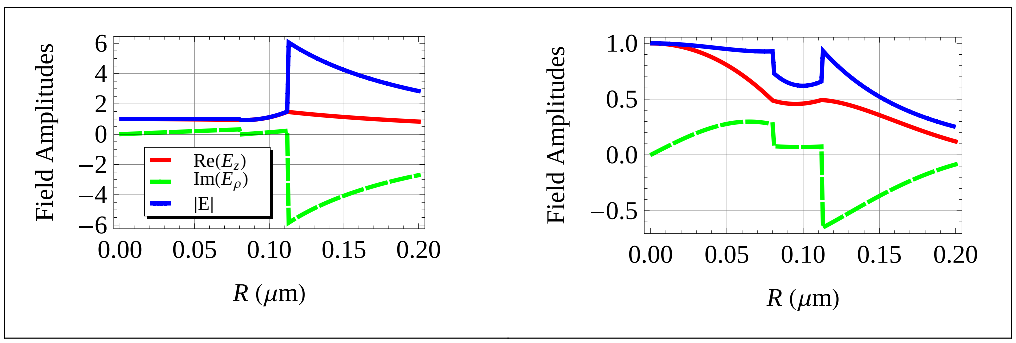

Fig. 8.28. SP fields for the lower energy mode (left) and the higher energy mode (right) of the gold cylindrical shell in Fig. 8.28. (*Mathematica* simulation)

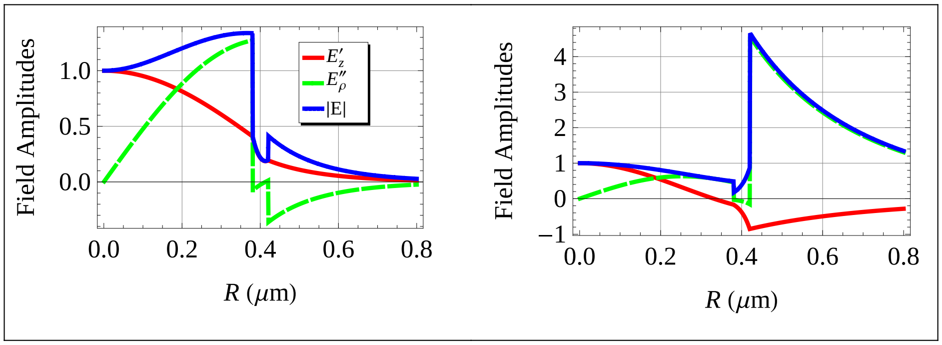

Fig. 8.29. SP fields for a gold cylindrical tube with an inner diameter of 380 nm and an outer diameter of 420 nm. The core is filled with a dielectric of relative permittivity 2.0 and the cylinder is surrounded on the outside by air. A mode with no zero crossing in E_z and with n_{eff} = 1.29+i 0.00876 is graphed on the left. A mode with a single zero crossing in E_z and with n_{eff} = 1.040+i 0.00211 is graphed on the right. (*Mathematica* simulation)

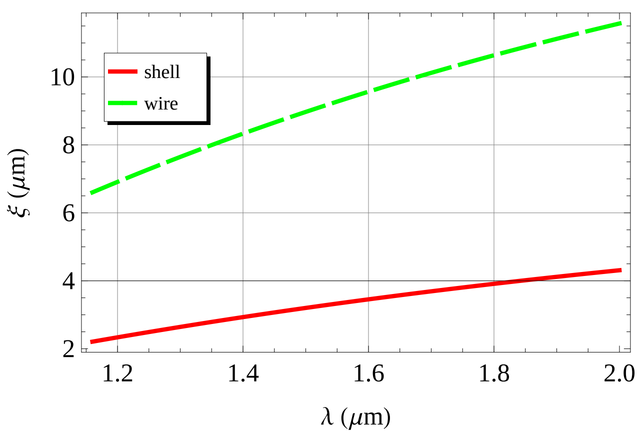

Fig. 8.30. Comparison of the 1/*e* propagation distance, ξ, of a SP on a solid cylindrical silver nanowire and a cylindrical silver shell filled with silica and surrounded by air as a function of wavelength, λ. The wire diameter and outer cylinder diameter is 50 nm. The inner cylinder diameter is 40 nm. (*Mathematica* simulation)

8.6 Excitation of surface plasmons on nanowires with plane waves

8.6.1 General solution

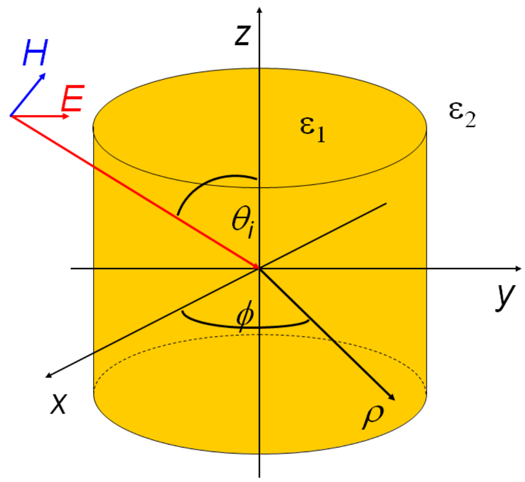

Fig. 8.31. Incident plane wave lies in *xz* plane with the *E* field along the *y*-direction and *H* field in the *xz* plane. The angle of incidence with respect to the axis of the cylindrical nanowire is θ_i. The azimuthal angle around the nanowire is ϕ, and the radial distance is ρ.

8.6.2 Nonpropagating surface plasmons

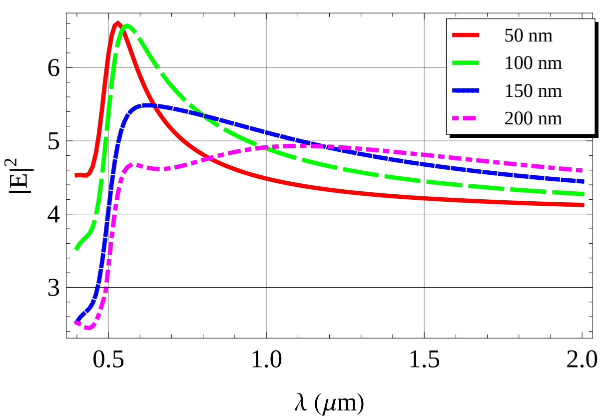

Fig. 8.32. Peak electric field intensity at the surface of gold cylindrical nanowires with diameters of 50, 100, 150, and 200 nm as a function of wavelength, λ, when excited by a plane wave of unit amplitude with wavevector orthogonal to the nanowire. (*Mathematica* simulation)

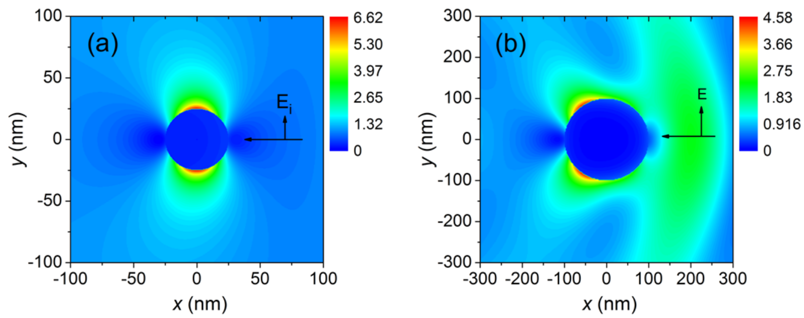

Fig. 8.33. Field intensity for a SP excited by an incident plane wave of unit amplitude on a gold cylindrical nanowire with a diameter of (a) 50 nm at a wavelength of 530 nm, and (b) 200 nm at a wavelength of 550 nm.

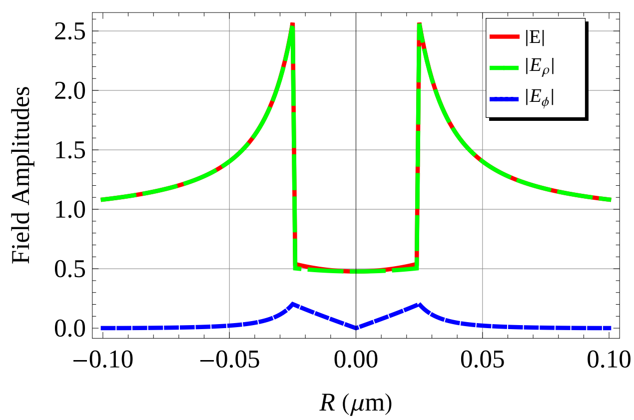

Fig. 8.34. Electric field intensity around a gold cylindrical nanowire with a radius of 25 nm at a wavelength of 530 nm as a function of radial position. |E| (solid line) and $|E_\rho|$ (dashed line) essentially overlap. (*Mathematica* simulation)

8.6.3 Scattering and absorption coefficients

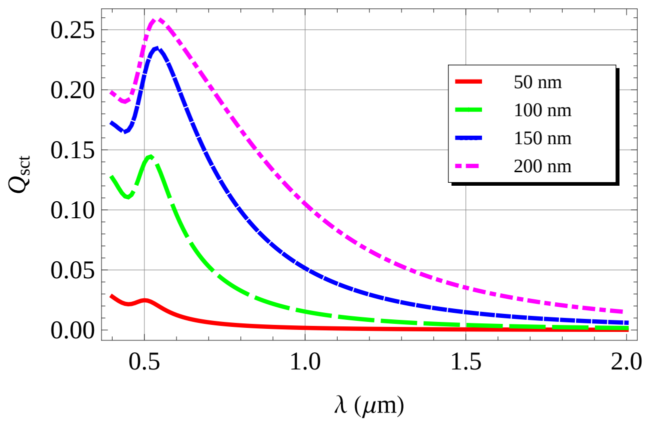

Fig. 8.35. Scattering efficiency from gold cylindrical nanowires with diameters of 50 nm (solid line), 100 nm (long dashes), 150 nm (short dashes), and 200 nm (dot dashes) as a function of wavelength, λ. (*Mathematica* simulation)

8.7 Nanowires with noncircular cross sections

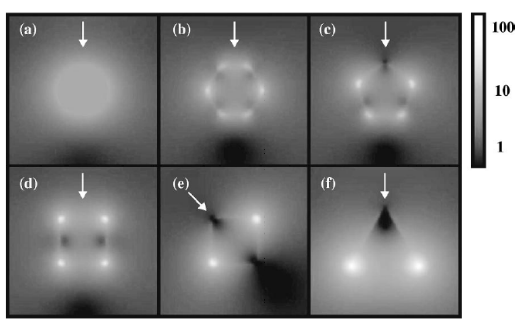

Fig. 8.36. Numerical simulations of a variety of nanowire shapes with a fixed cross sectional area equal to that of the circular wire (a) with a 20 nm diameter. The white arrow indicates the direction of propagation of the incident plane wave. Reprinted with permission from J.P.Kottmann *et al.*, *Phys. Rev. B* **64** 235402 (2001). © 2001 by the American Physical Society. [31]

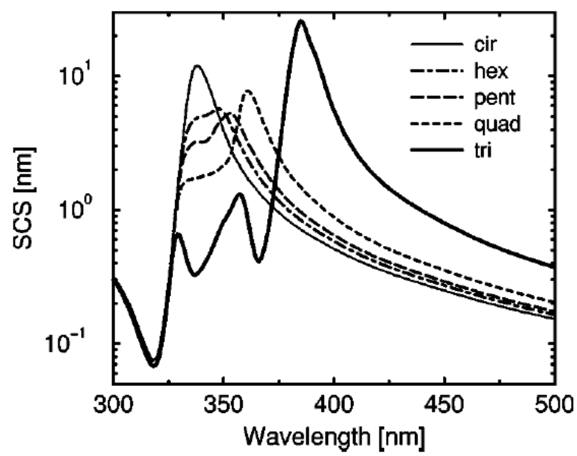

Fig. 8.37. Scattering cross section vs. wavelength for a variety of nanowire shapes with fixed cross sectional areas equal to that of the circular wire with a 20 nm diameter. Reprinted with permission from J.P.Kottmann *et al.*, *Phys. Rev. B* **64** 235402 (2001). © 2001 by the American Physical Society. [31]

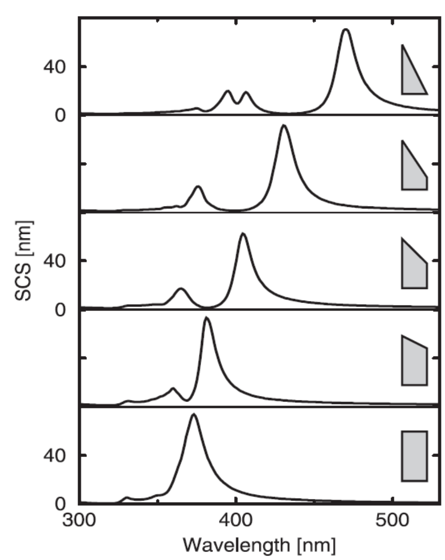

Fig. 8.38. Scattering cross section calculated for a silver nanowire with a cross section that varies from triangular to rectangular with dimensions of 17 nm × 34 nm. Reprinted with permission from J. P. Kottmann and O. J. F. Martin, *Appl. Phys. B* **73** 299-304 (2001). © 2001 by the American Physical Society. [32]

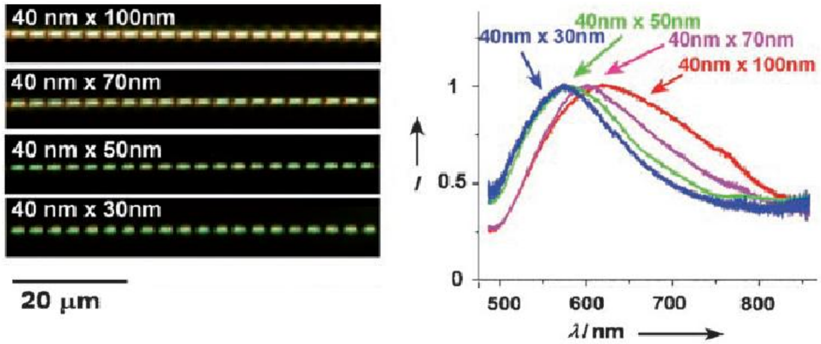

Fig. 8.39. (Left) Dark field images of 2 μm gold nanowires. The horizontal by vertical cross sectional areas are indicated. (Right) Scattered spectra exhibiting a SP resonance. Q. Xu, J. Bao, F. Capasso, and G. M. Whitesides, "Surface Plasmon Resonances of Free-Standing Gold Nanowires Fabricated by Nanoskiving," *Angew. Chem.* (2006) **118** 3713-3717 © Wiley-VCH Verlag GmbH & Co. KGaA. Reproduced with permission.

Exercises

1. How does the propagation distance for a silver nanowire compare to that for a gold nanowire? Plot the propagation distance as a function of cylinder radius from 10 to 100 nm at a wavelength of 532 nm and 820 nm.

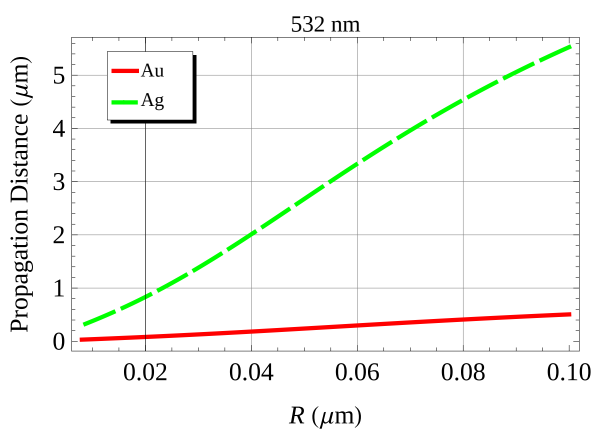

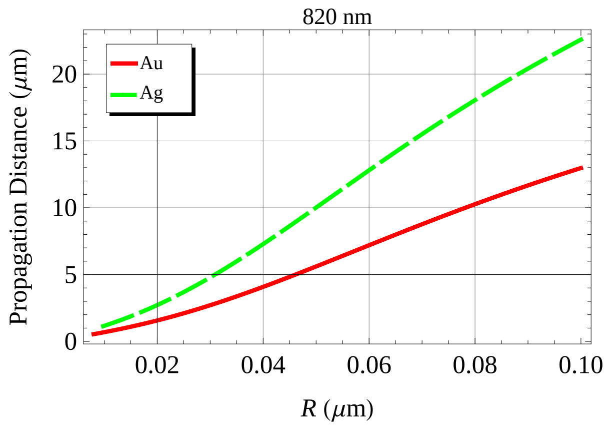

2. An example was given (Fig. 8.29) of two n = 0 modes for a cylindrical tube at the same frequency, one of which exhibited the same surface charge polarity on the inner and outer surfaces and one of which exhibited opposite surface charge polarity. Consider the example of a silver tube with an inner *diameter* of 1 μm and an outer *diameter* of 1.1 μm at a free space wavelength of 633 nm. Plot the fields for the first two modes as a function of radial position (hint: for one mode try an initial SP effective index of 1.6 and for the other mode try an initial SP index of 1.1). Are the surface charges of the same sign or opposite sign on the inner and outer surfaces of the tube for each mode?

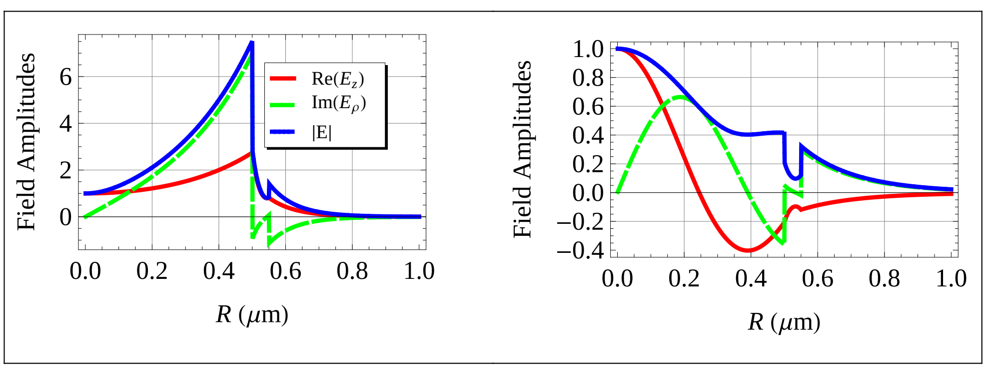

References

[1] C. A. Pfeiffer, E. N. Economou and K. L. Ngai. Surface polaritons in a circularly cylindrical interface: surface plasmons. *Phys. Rev. B* **10** (1974) 3038.

[2] J. Takahara, S. Yamagishi, H. Taki, A. Morimoto and T. Kobayashi. Guiding of a one-dimensional optical beam with nanometer diameter. *Opt. Lett.* **22** (1997) 475.

[3] H. Khosravi, D. R. Tilley and R. Loudon. Surface polaritons in cylindrical optical fibers. *J. Opt. Soc. Am A* **8** (1991) 112.

[4] U. Schröter and A. Dereux. Surface plasmon polaritions on metal cylinders with dielectric core. *Phys. Rev. B* **64** (2001) 125420.

[5] C. Miziumski. Utilization of a cylindrical geometry to promote radiative interaction with slow surface excitations. *Phys. Lett.* A **40** (1972) 187.

[6] P. Berini. Plasmon-polariton modes guided by a metal film of finite width. *Opt. Lett.* **24** (1999) 1011.

[7] P. Berini. Plasmon-polariton waves guided by thin lossy metal films of finite width: bound modes of symmetric structures. *Phys. Rev. B* **61** (2000) 10484.

[8] I. Breukelaar, R. Charbonneau and P. Berini. Long-range surface plasmon-polariton mode cutoff and radiation in embedded strip waveguides. *J. Appl. Phys.* **100** (2006) 043104.

[9] R. Zia, M. D. Selker and M. L. Brongersma. Leaky and bound modes of surface plasmon waveguides. *Phys. Rev. B* **71** (2005) 165431.

[10] R. M. Dickson and L. A. Lyon. Unidirectional Plasmon Propagation in Metallic Nanowires. *J. Phys. Chem. B* **104** (2000) 6095.

[11] J-C. Weeber, A. Dereux, C. Girard, J. R. Krenn and J-P. Goudonnet. Plasmon polaritons of metallic nanowires for controlling submicron propagation of light. *Phys. Rev. B* **60** (1999) 9061.

[12] J. R. Krenn, B. Lamprecht, H. Ditlbacher, G. Schider, M. Salerno, A. Leitner and

F. R. Aussenegg. Non-diffraction-limited light transport by gold nanowires. *Europhys. Lett.* **60** (2002) 663.

[13] B. Lamprecht, J. R. Krenn, H. Ditlbacher, M. Salerno, N. Felidj, A. Leitner, F. R. Aussenegg and J. C. Weeber. Surface plasmon propagation in microscale metal stripes. *Appl. Phys. Lett.* **79** (2001) 51.

[14] H. Ditlbacher, A. Hohenau, D. Wagner, U. Kriebig, M. Rogers, F. Hofer, F. R. Aussenegg and J. R. Krenn. Silver nanowires as surface plasmon resonators. *Phys. Rev. Lett.* **95** (2005) 257403.

[15] R. Zia, J. A. Schuller and M. L. Brongersma. Near-field characterization of guided polariton propagation and cutoff in surface plasmon waveguides. *Phys. Rev. B* **74** (2006) 165415.

[16] T. Nikolajsen, K. Leosson, I. Salakhutdinov and S. I. Bozhevolnyi. Polymer-based surface-plasmon-polariton stripe waveguides at telecommunication wavelengths. *Appl. Phys. Lett.* **82** (2003) 668.

[17] T. Nikolajsen, K. Leosson and S. Bozhevolni. Surface plasmon polariton based modulators and switches operating at telecom wavelengths. *Appl. Phys. Lett.* **85** (2004) 5833.

[18] N. C. J. van der Valk and P. C. M. Planken. Effect of dielectric coating on tera-hertz surface plasmon polaritons on metal wires. *Appl. Phys. Lett.* **87** (2005) 071106.

[19] B. Steinberger, A. Hohenau, H. Ditlbacher, A. L. Stepanov, A. Drezet, F. R. Aussenegg, A. Leitner and J. R. Krenn. Dielectric stripes on gold as surface plasmon waveguides. *J. Appl. Phys.* **88** (2006) 094104.

[20] J. Q. Lu and A. A. Maradudin. Channel plasmons. *Phys. Rev. B* **42** (1990) 11159.

[21] I. V. Novikov and A. A. Maradudin. Channel polaritons. *Phys. Rev. B* **66** (2002) 035403.

[22] D. F. P. Pile and D. K. Gramotnev. Plasmonic subwavelength waveguides: next to zero losses at sharp bends. *Opt. Lett.* **30** (2005) 1186.

[23] S. Bozhevolyni, V. S. Volkov, E. Devaux, J-Y. Laluet and T. W. Ebbesen. Channel plasmon subwavelength waveguide components including interferometers and ring

resonators. *Nature* **440** (2006) 508.

[24] E. C. Jordan and K. G. Balmain. *Electromagnetic Waves and Radiating Systems* (Englewood Cliffs, Prentice-Hall, 1968) Chap. 8.

[25] L.Novotny and C. Hafner. Light propagation in a cylindrical waveguide with a complex, metallic, dielectric function. *Phys. Rev. E* **50** (1994) 4094.

[26] H. Shin, P. B. Catrysse and S. Fan. Effect of the plasmonic dispersion relation on the transmission properties of subwavelength cylindrical holes. *Phys. Rev. B* **72** (2005) 85436.

[27] M. Abramowitz and I. A. Stegun. *Handbook of Mathematical Functions* (New York, Dover, 1972).

[28] C. F. Bohren and D. R. Huffman. *Absorption and Scattering of Light by Small Particles* (New York, Wiley, 1998) Chap. 8.

[29] R. D. Birkhoff, J. C. Ashley, H. H. Hubbell, Jr., and L. C. Emerson. Light scattering from micron-size fibers. *J. Opt. Soc. Am.* **67** (1977) 564.

[30] J. P. Kottmann, O. J. F. Martin, D. R. Smith and S. Schultz. Dramatic localized electromagnetic enhancement in plasmon resonant nanowires. *Chem. Phys. Lett.* **341** (2001) 1.

[31] J. P. Kottmann, O. J. F. Martin, D. R. Smith and S. Schultz. Plasmon resonances of silver nanowires with a nonregular cross section. *Phys. Rev. B* **64** (2001) 235402.

[32] J. P. Kottmann and O. J. F. Martin. Influence of the cross section and the permittivity on the plasmon-resonance spectrum of silver nanowires. *Appl. Phys. B* **73** (2001) 299.

[33] Q. Xu, J. Bao, F. Capasso and G. M. Whitesides. Surface plasmon resonances of free-standing gold nanowires fabricated by nanoskiving. *Angew. Chem.* **118** (2006) 3713.

[34] V. Giannini and J. A. Sánchez-Gil. Calculations of light scattering from isolated and interacting metallic nanowires of arbitrary cross section by means of Green’s theorem surface integral equations in parametric form. *J. Opt. Soc. Am. A* **24** (2007) 2822.